Preparation, Characterization, and X-ray Crystal Structures of Helical and Syndiotactic Zinc-Based Coordination Polymers

William W. Ellis, Marion Schmitz, Atta A. Arif, and Peter J. Stang*

Department of Chemistry, University of Utah, Salt Lake City, Utah 84112

Received November 10, 1999

The reactions of $(facac)_2Zn{\cdot}2H_2O$ (facac = 1,1,1,5,5,5-hexafluoroacetylacetonate) with 2,5-bis(4-ethynylpyridyl)-furan (**1**) and 1,2-bis(4-ethynylpyridyl)benzene (**2**) yield, upon crystallization, coordination polymers. The former polymer, $\{(facac)_2Zn{\cdot}\mathbf{1}\}_n$, has an isotactic, helical structure in the solid state [monoclinic space group $P2_1/n$; a = 11.0374(3) Å, b = 24.2179(10) Å, c = 14.3970(4) Å, β = 92.880(2)°; Z = 4]. The latter polymer, $\{(facac)_2Zn{\cdot}\mathbf{2}\}_n$, adopts a syndiotactic structure in the solid state [monoclinic space group $P2_1/n$; a = 9.1344(1) Å, b = 21.7985(5) Å, c = 16.0322(4) Å, β = 99.6680(11)°; Z = 4]. The solution structures of the corresponding oligomers have been studied by low-temperature ^{1}H and ^{19}F NMR spectroscopy. Chiral polymers were prepared using the fragment $[(+)\text{-tfc}]_2Zn$ ((+)-tfc = 3-((trifluoromethyl)hydroxymethylene)-(+)-camphorate). A linear, zigzag structure was found for $\{[(+)\text{-tfc}]_2Zn{\cdot}\mathbf{1}\}_n$ [triclinic space group $P1$; a = 7.4833(2) Å, b = 14.1563(5) Å, c = 21.21230(5) Å, α = 78.4440(15)°, β = 81.5644(15)°, γ = 76.4976(13)°; Z = 1]. Reaction with tris(4-pyridyl)methanol (**3**) yielded a homochiral, helical polymer, $\{[(+)\text{-tfc}]_2Zn{\cdot}\mathbf{3}\}_n$ [monoclinic space group $C2$; a = 25.0633(12) Å, b = 11.8768(7) Å, c = 17.1205(9) Å, α = 90°, β = 117.954(3)°, γ = 90°; Z = 4].

Introduction

Coordination-driven self-assembly has been used to prepare a wide variety of discrete supramolecular species.[1−3] Likewise, many highly ordered coordination polymers and polymeric networks have been prepared by relatively simple self-assembly reactions.[4−6] Metal-containing polymers are of fundamental interest because of their promising magnetic, optical, electrical, and mechanical properties, as well as combinations of the aforementioned.[4,7]

Of particular interest, and relevance to this paper, are chiral self-assembled systems, especially systems derived from prochiral metal fragments which act as connecting units or templates. Despite the complexity that this adds to the self-assembly process, due to the possible formation of diastereomers, many discrete supramolecular species have been prepared that incorporate multiple homochiral metal centers. Notable examples include both linear and cyclic helicates prepared by Lehn,[1,8,9] tetrahedral clusters prepared by both Saalfrank[10] and Raymond,[11] and a remarkable cubic cluster prepared by Robson[12] which is constructed from 12 homochiral, tetragonal copper centers. Several isotactic polymers have also been prepared through self-assembly. These include helical coordination polymers prepared by Gatteschi,[13] Inoue,[14] and Iwamura.[15] Helical coordination polymers which spontaneously resolve to produce enantiomorphic crystals have been prepared by both Aoyama[16] and Zawarotko.[17] Syndiotactic systems are less common. Linear hydrogen-bonded syndiotactic polymers have been prepared by Matsumoto,[18] and examples of two- and three-dimensional polymeric arrays with syndiotactic repeat units have been prepared by Iwamura.[15]

This paper reports first the reaction of the neutral, cis-binding zinc fragment $(facac)_2Zn$ (facac = 1,1,1,5,5,5-hexafluoroacetylacetonate)[19] with two different bis(pyridyl) linkers. The linkers are angular, with expected bite angles of 140 and 60°. Changing the bite angle of the linking group changes the architecture and the microstructure of the resultant crystalline polymers. When the metal centers are connected by the broader of the two ligands, an isotactic, helical polymer is obtained. There is much current interest in the designed synthesis of helical oligomers and polymers.[20−29] On the other hand, the narrower linker produces a wedge-shaped, syndiotactic polymer.

(1) Lehn, J.-M. *Angew. Chem., Int. Ed. Engl.* **1990**, *29*, 1304.
(2) Fujita, M.; Ogura, K. *Coord. Chem. Rev.* **1996**, *148*, 249.
(3) Leininger, S.; Olenyuk, B.; Stang, P. J. *Chem. Rev.* **2000**, *100*, 853.
(4) Chen, C.; Suslick, K. S. *Coord. Chem. Rev.* **1993**, *128*, 293.
(5) Robson, R. *Compr. Supramol. Chem.* **1997**, *6*, 733.
(6) Withersby, M. A.; Blake, A. J.; Champness, N. R.; Cooke, P. A.; Hubberstey, P.; Li, W.; Schroder, M. *Inorg. Chem.* **1999**, *38*, 2259.
(7) Nguyen, P.; Gomez-Elipe, P.; Manners, I. *Chem. Rev.* **1999**, *99*, 1515.
(8) Hasenkopf, B.; Lehn, J.-M.; Baum, G.; Kneisel, B. O.; Fenske, D. *Angew. Chem., Int. Ed. Engl.* **1996**, *34*, 1838.
(9) Hasenkopf, B.; Lehn, J.-M.; Boumediene, N.; Dupont-Gervais, A.; van Dorsselaer, A.; Kneisel, B.; Fenske, D. *J. Am. Chem. Soc.* **1997**, *119*, 10596.
(10) Saalfrank, R. W.; Burak, R.; Breit, A.; Stalke, D.; Herbst-Irmer, R.; Daub, J.; Borsh, M.; Bill, E.; Muthe, M.; Trautwein, A. X. *Angew. Chem., Int. Ed. Engl.* **1994**, *33*, 1621.
(11) Caulder, D. L.; Raymond, K. N. *J. Chem. Soc., Dalton Trans.* **1999**, 1185.
(12) Abrahams, B. F.; Egan, S. J.; Robson, R. *J. Am. Chem. Soc.* **1999**, *121*, 3535.
(13) Caneschi, A.; Gatteschi, D.; Rey, P.; Sessoli, R. *Inorg. Chem.* **1991**, *30*, 3936.
(14) Kumagi, H.; Inoue, K. *Angew. Chem., Int. Ed. Engl.* **1999**, *38*, 1601.
(15) Iwamura, H.; Inoue, K.; Koga, N. *New J. Chem.* **1998**, 201.
(16) Ezuhara, T.; Endo, K.; Aoyama, Y. *J. Am. Chem. Soc.* **1999**, *121*, 3279.
(17) Biradha, K.; Seward, C.; Zawarotko, M. J. *Angew. Chem., Int. Ed. Engl.* **1999**, *38*, 492.
(18) Shii, Y.; Motoda, Y.; Matsuo, T.; Kai, F.; Nakashima, T.; Tuchagues, J.-P.; Matsumoto, M. *Inorg. Chem.* **1999**, *38*, 3513.
(19) Pradilla-Sorzano, J.; Fackler, J. P. *Inorg. Chem.* **1973**, *12*, 1973.
(20) Nuckolls, C.; Katz, T. J.; Katz, G.; Collings, P. J.; Castellanos, L. *J. Am. Chem. Soc.* **1999**, *121*, 79.
(21) Bassani, D. M.; Lehn, J.-M.; Baum, G.; Fenske, D. *Angew. Chem., Int. Ed. Engl.* **1997**, *36*, 1845.
(22) Gin, M. S.; Yokozawa, T.; Prince, R. B.; Moore, J. S. *J. Am. Chem. Soc.* **1999**, *121*, 2643.

10.1021/ic991315m CCC: $19.00
Published on Web 05/13/2000

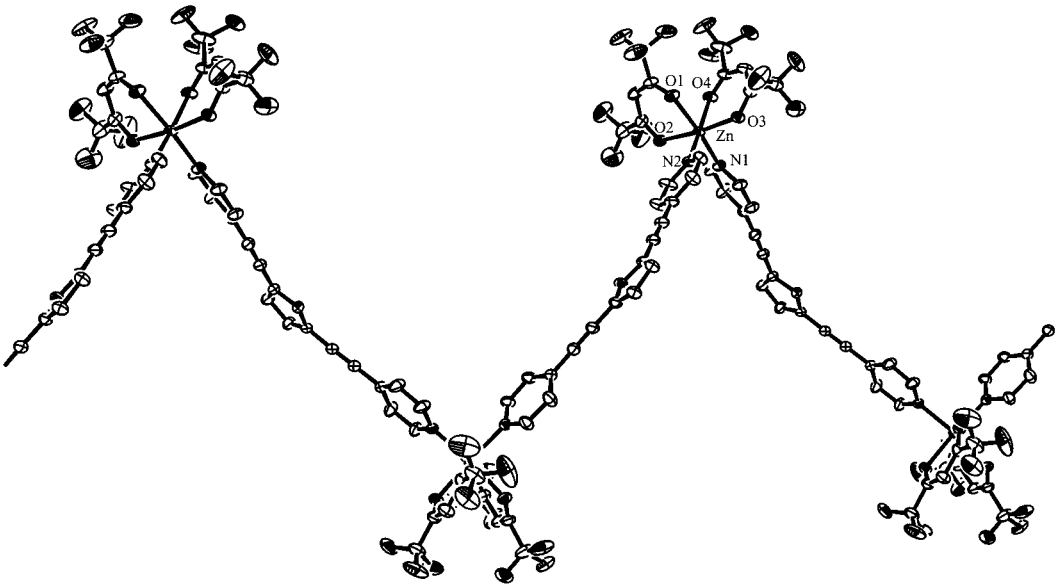

Figure 1. ORTEP diagram of (*S*)-{(facac)$_2$Zn·**1**}$_n$ with 25% thermal ellipsoids. For clarity, H atoms have been omitted and only one orientation of F atoms has been shown.

Furthermore, a homochiral helical polymer is reported. To that end, the chiral zinc linker [(+)-tfc]$_2$Zn was prepared ((+)-tfc = 3-((trifluoromethyl)hydroxymethylene)-(+)-camphorate). This unit was in turn combined with two different organic linkers, in one case producing the desired right-handed helical polymer.

Results

Bis(pyridyl) compounds **1** and **2** were prepared as shown in eqs 1 and 2 by standard palladium-catalyzed coupling of 4-ethynylpyridine with the respective dihalide.[30] Each has been

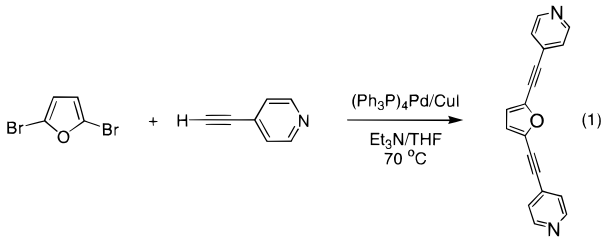

1
67% yield

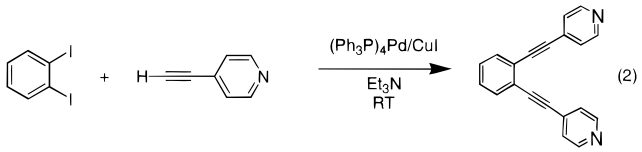

2
67% yield

characterized by both ^{1}H and ^{13}C NMR spectroscopy and elemental analysis. In addition, crystals of **1** grown from acetone were analyzed by X-ray diffraction. Crystallographic information is given in the Supporting Information. The most noteworthy finding is that the bite angle of this molecule is 127°, which is significantly smaller than anticipated (140−144°). There is no distortion evident in the molecule due to an inward bending around the acetylenic bridges. However, as will be shown later, this bite angle can distort on coordination to a zinc complex.

Furanyl linker **1** was first reacted with commercially available (facac)$_2$Zn·2H$_2$O in an NMR tube in acetone-d_6. Release of the coordinated aquo groups was evident, due to the upfield shift in the ^{1}H NMR resonance of the water signal. Likewise, downfield shifts were observed for the β-hydrogens of the pyridyl groups of **1**, as well as for the furanyl hydrogen. There was no change in the chemical shift of the α-hydrogens of the pyridyl groups of **1** or in the chemical shift of the singlet corresponding to the 3-H of the facac groups. The ^{19}F NMR spectrum showed a singlet at −76.6 ppm, which was unshifted relative to that of the starting aquo complex. The simplicity of the ^{19}F NMR spectrum suggests that this system is under dynamic equilibrium on the NMR time scale. The anticipated cis binding of the pyridyl groups should produce two singlets in the ^{19}F spectrum due to quasi-axial and equatorial positions for the CF_3 groups. Low-temperature NMR experiments on this, and related materials, will be discussed in a further section.

Crystals of {(facac)$_2$Zn·**1**}$_n$ were grown from a mixture of toluene and acetone. When removed from the mother liquor, the crystals quickly effluoresced, becoming opaque and brittle and soon collapsing into a white powder. When coated with a viscous oil, they were sufficiently stable for crystallographic analysis. The structure was solved as described in the Experimental Section.

As shown in Figures 1 and 2, the polymer adopts a helical structure in the solid state. The polymer crystallizes in the centrosymmetric space group $P2_1/n$, and subsequently both *R*- and *S*-helixes are present in equal amounts (see Table 1). Figure 2 shows a horizontal view of the polymer chain. In this case,

(23) Prince, R. B.; Saven, J. G.; Wolynes, P. G.; Moore, J. S. *J. Am. Chem. Soc.* **1999**, *121*, 3114.
(24) Rowan, A. E.; Nolte, R. J. M. *Angew. Chem., Int. Ed. Engl.* **1998**, *37*, 63.
(25) Jha, S. K.; Cheon, K.-S.; Green, M. M.; Selinger, J. V. *J. Am. Chem. Soc.* **1999**, *121*, 1665.
(26) Englekamp, H.; Middlebeek, S.; Nolte, R. J. M. *Science* **1999**, *284*, 785.
(27) Bowyer, P. K.; Porter, K. A.; Rae, A. D.; Willis, A. C.; Wild, S. B. *J. Chem. Soc., Chem. Commun.* **1998**, 1153.
(28) Withersby, M. A.; Blake, A. J.; Champness, N. R.; Hubberstey, P.; Li, W.-S.; Schroder, M. *Angew. Chem., Int. Ed. Engl.* **1997**, *36*, 2327.
(29) Wu, B.; Zhang, W.-J.; Yu, S.-Y.; Wu, X.-T. *J. Chem. Soc., Dalton Trans.* **1997**, 1795.
(30) Takahashi, S.; Kuroyama, Y.; Sonogashira, K.; Hagihara, N. *Synthesis* **1980**, 627.

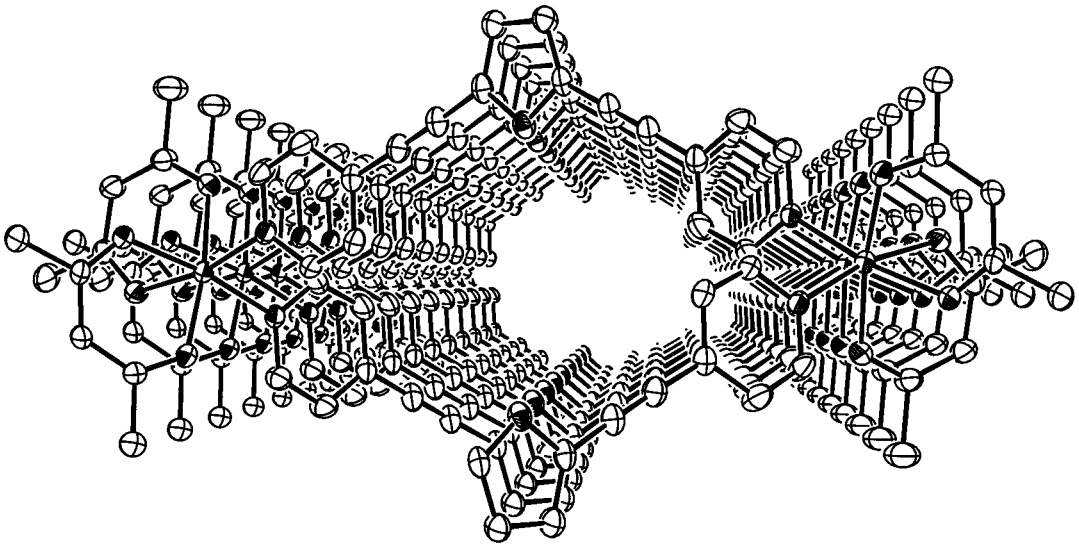

Figure 2. View of (*S*)-{(facac)$_2$Zn·**1**}$_n$ down the polymer axis. H and F atoms have been omitted for clarity.

Table 1. Crystallographic Data for {(facac)$_2$Zn·**1**}$_n$

empirical formula	$C_{34}H_{18}F_{12}N_2O_5Zn$
fw	827.87
temperature	200(0.1) K
wavelength	0.710 73 Å
crystal system	monoclinic
space group	$P2_1/n$
unit cell dimensions	a = 11.0374(3) Å, b = 24.2179(10) Å, c = 14.3970(4) Å, α = 90°, β = 92.880(2°), γ = 90°
volume	3843.5(2) Å^3
Z	4
density (calcd)	1.431 Mg/m^3
abs coeff	0.737 mm^{-1}
θ range for data collection	3.71−25.95°
final R indices [$I > 2\sigma(I)$][a]	R1 = 0.0632, wR2 = 0.1617
R indices (all data)[a]	R1 = 0.1005, wR2 = 0.1852

[a] $R1 = \sum||F_o| - |F_c||/\sum|F_o|$; $wR2 = [\sum w(F_o^2 - F_c^2)^2/\sum w(F_o^2)^2]^{1/2}$.

Table 2. Selected Bond Lengths (Å) and Angles (°) for {(facac)$_2$Zn·**1**}$_n$

Zn−N1	2.110(4)	Zn−O1	2.138(3)	Zn−O3	2.062(3)
Zn−N2	2.114(4)	Zn−O2	2.089(3)	Zn−O4	2.146(3)
	N1−Zn−N2			94.90(14)	

the *S*-helix is shown. Each revolution of the helix requires two symmetry-related (facac)$_2$Zn·**1** units. The chirality at each metal center in the *S*-helix is Λ. Likewise, for the *R*-helices, the chirality about the metal centers is Δ. The distance between subsequent turns in the helix is 24.2 A.

The coordination environment about each zinc atom (Table 2) is similar to that found previously for (facac)$_2$Zn·2py (py = pyridine).[19] The N1−Zn−N2 angle is somewhat smaller in the polymer than in (facac)$_2$Zn·2py, 94.9° vs 99.0°. The facac binding in the polymer is unsymmetrical, as was found for the monomer (facac)$_2$Zn·2py. The Zn−O bonds trans to the pyridyl groups are ∼0.07 Å longer than those cis to the pyridyl groups. In the monomer, this difference is ∼0.09 Å. The bite angle of the coordinated ligand **1** is 132°. This angle is ∼5° larger than that found for the free ligand.

The view down the polymer axis (Figure 2) shows that a channel with approximately 7.7 × 12.1 Å dimensions exists within the polymer coil. The channel is not empty, however. It is occupied by fragments of adjacent, parallel polymer coils. Still, there are significant channels within the crystal, as seen in a view normal to the (010) plane of the unit cell (Figure 3). These channels are occupied by disordered toluene molecules (only one channel is shown bearing these solvent molecules). The approximate horizontal dimensions of the channels are 7.6 × 11.8 Å.

Table 3. Crystallographic Data for {(facac)$_2$Zn·**2**}$_n$

empirical formula	$C_{30}H_{14}F_{12}N_2O_4Zn$
fw	759.80
temperature	200(0.1) K
wavelength	0.710 73 Å
crystal system	monoclinic
space group	$P2_1/n$
unit cell dimensions	a = 9.13440(10) Å, b = 21.7985(5) Å, c = 16.0322(4) Å, α = 90°, β = 99.6680(11)°, γ = 90°
volume	3146.93(11) Å^3
Z	4
density (calcd)	1.604 Mg/m^3
abs coeff	0.890 mm^{-1}
θ range for data collection	3.35−30.04°
final R indices [$I > 2\sigma(I)$][a]	R1 = 0.0464, wR2 = 0.0984
R indices (all data)[a]	R1 = 0.0852, wR2 = 0.1127

[a] $R1 = \sum||F_o| - |F_c||/\sum|F_o|$; $wR2 = [\sum w(F_o^2 - F_c^2)^2/\sum w(F_o^2)^2]^{1/2}$.

Subsequently, the 60° linker **2** was reacted with (facac)$_2$Zn·2H$_2$O. Observations made in the ^{1}H and ^{19}F NMR spectra were similar to those described above for {(facac)$_2$Zn·**1**}$_n$. Colorless crystals were grown by storing a vial holding an acetone solution of {(facac)$_2$Zn·**2**}$_n$ in a jar of pentane for several days. These crystals were stable when removed from the mother liquor and did not decompose even when placed under vacuum for several hours.

The structure of {(facac)$_2$Zn·**2**}$_n$ was solved as described in the Experimental Section. As in the previous case, a coordination polymer was obtained, which crystallized in the space group $P2_1/n$ (see Table 3). Two different views of the polymer are given in Figures 4 and 5.

The structure of {(facac)$_2$Zn·**2**}$_n$ contrasts nicely with that of {(facac)$_2$Zn·**1**}$_n$. As opposed to the isotactic, helical structure of the former polymer, the structure of {(facac)$_2$Zn·**2**}$_n$ is syndiotactic. Successive metal centers display opposite chiralities. Centers with Λ-chirality initiate a right-handed turn in the polymer. A full helix is not obtained, as the subsequent metal center with Δ-chirality initiates a left-handed helical turn, producing the wedge-shaped polymer shown in Figure 5 looking down the axis. There are no substantial channels within the crystal, and solvent was not retained during crystallization.

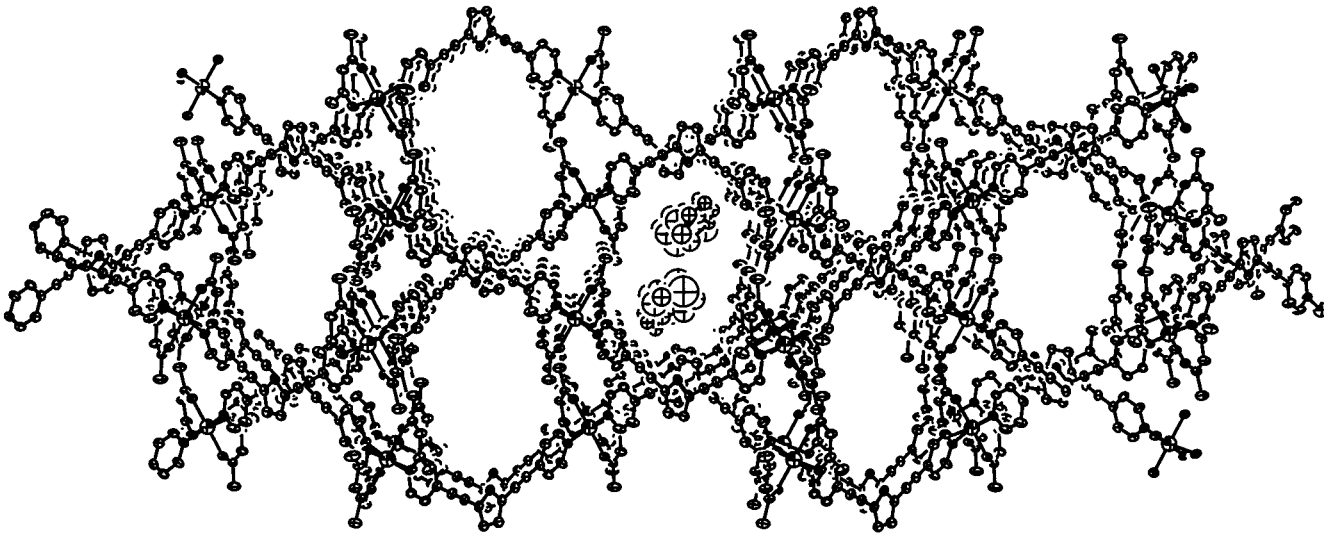

Figure 3. View of the unit cell of $\{(facac)_2Zn\cdot\mathbf{1}\}_n$ normal to the (100) plane. Solvent molecules are shown in the central cavity only, and H and F atoms have been omitted for clarity.

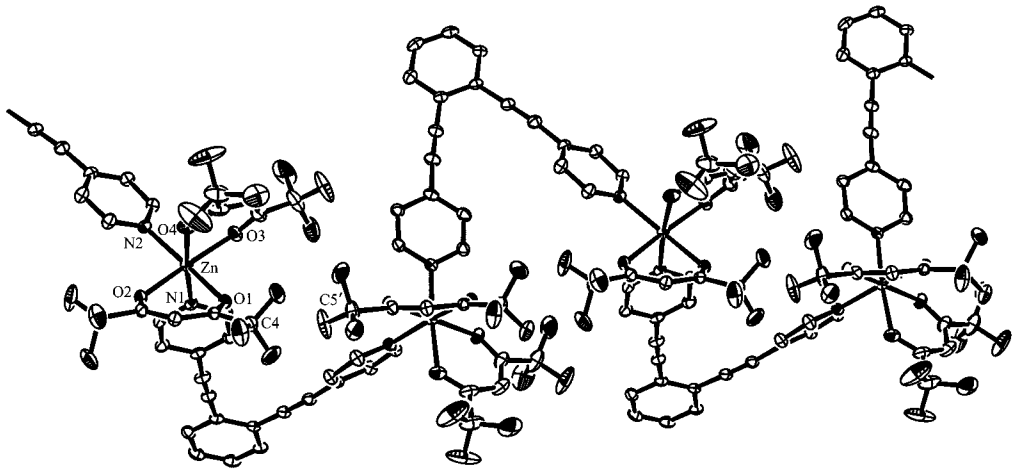

Figure 4. ORTEP diagram of $\{(facac)_2Zn\cdot\mathbf{2}\}_n$ with 25% thermal ellipsoids. For clarity, H atoms have been omitted, and only a single orientation of F atoms has been shown.

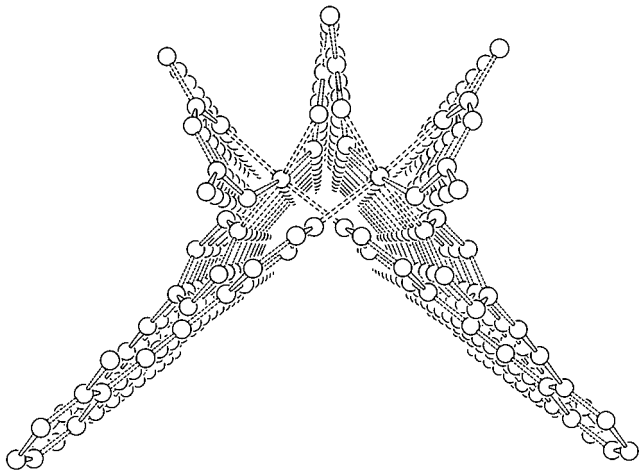

Figure 5. View of $\{(facac)_2Zn\cdot\mathbf{2}\}_n$ down the polymer axis. H and F atoms have been omitted for clarity.

The coordination environment about the zinc centers (Table 4) is similar to that found for the helical polymer. The N1−Zn−N2 angle is 97.1°. Surprisingly, the bite angle of the linker **2** is 51°. This is significantly less than expected. As a result, the C4−C5′ separation of trifluoromethyl groups on adjacent zinc centers is quite close, at 4.10 Å (see Figure 4).

Table 4. Selected Bond Lengths (Å) and Angles (deg) for $\{(facac)_2Zn\cdot\mathbf{2}\}_n$

Zn−N(1)	2.097(2)	Zn−O(1)	2.160(1)	Zn−O(3)	2.060(2)
Zn−N(2)	2.119(2)	Zn−O(2)	2.084(1)	Zn−O(4)	2.136(2)
N1−Zn−N2				97.06(2)	

Solution Studies. As noted above, both zinc polymers exhibit dynamic ^{1}H and ^{19}F NMR spectra in acetone-d_6 solution at room temperature. The monomeric complex $(facac)_2Zn\cdot 2py$ also shows dynamic NMR and will be discussed first.

When 3 equiv of pyridine is added to an acetone-d_6 solution of $(facac)_2Zn\cdot(H_2O)_2$, a single set of resonances due to pyridine are observed at room temperature. The resonances for the β- and γ-hydrogen atoms are shifted downfield relative to those of free pyridine, whereas the resonance for the α-hydrogen atoms is unshifted (see Figure 6). Again, there is a lone singlet in the ^{19}F NMR spectrum. When the sample is cooled to −80 °C, the equilibration is slowed and two bound pyridyl groups are evident, in addition to 1 equiv of free pyridine. There are two singlets of equal intensity in the ^{19}F NMR spectrum, which arise from the quasi-axial and equatorial CF_3 groups found in the cis complex (see Figure 7).

Both polymers, after crystallization, can be redissolved in acetone-d_6. The ^{19}F NMR spectrum of each polymer at −80

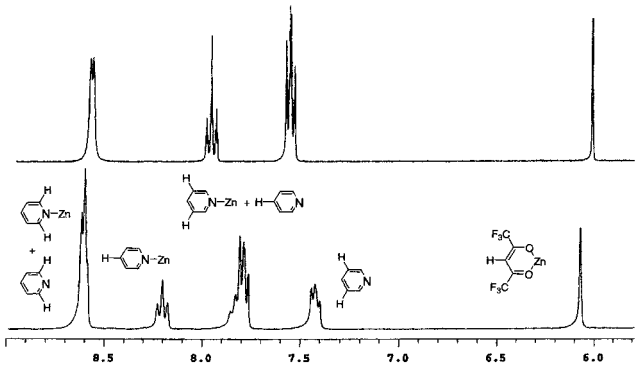

Figure 6. ^{1}H NMR spectra of (facac)$_2$Zn·2py + py in acetone-d_6 at 20 °C (above) and −80 °C (below).

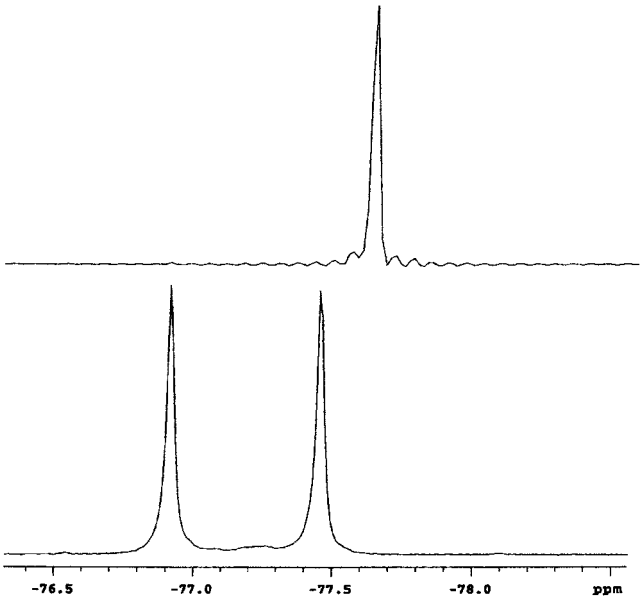

Figure 7. ^{19}F NMR spectra of (facac)$_2$Zn·2py + py in acetone-d_6 at 20 °C (above) and −80 °C (below).

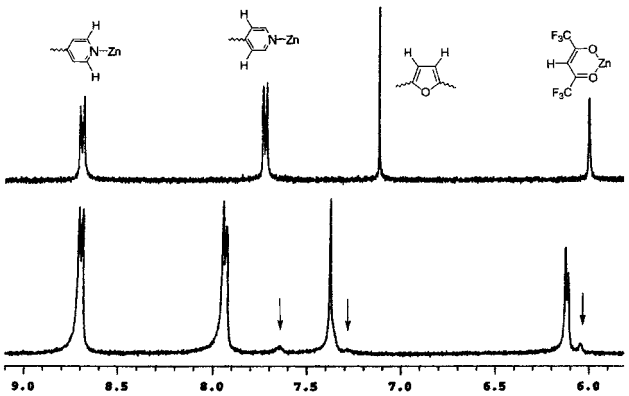

Figure 8. ^{1}H NMR spectra of {(facac)$_2$Zn·**1**}$_n$ in acetone-d_6 at 20 °C (above) and −80 °C (below). End groups are marked with arrows.

°C is similar to that described above for (facac)$_2$Zn·2py. This demonstrates the cis binding of the pyridyl groups to the zinc fragments in each case. The ^{1}H NMR spectrum of the helical polymer {(facac)$_2$Zn·**1**}$_n$ at −80 °C is more complicated (see Figure 8). On cooling, the resonance for the β-hydrogens of the pyridyl groups as well as the resonance of the furanyl hydrogen separate into two distinct resonances. Each minor resonance is shifted upfield relative to the major resonance and likely corresponds to the uncoordinated end groups of the oligomers present in solution. From a comparison of the relative

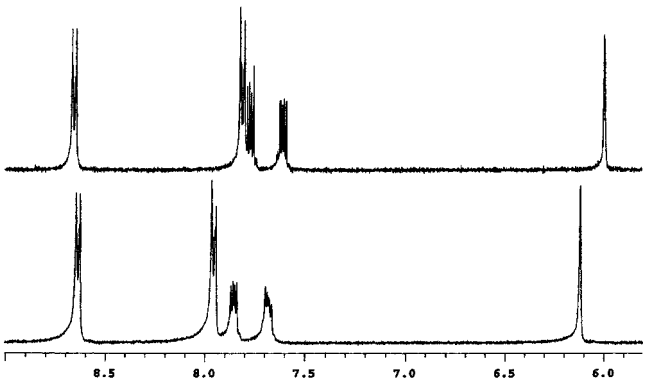

Figure 9. ^{1}H NMR spectra of {(facac)$_2$Zn·**2**}$_n$ in acetone-d_6 at 20 °C (above) and −80 °C (below).

intensities of the two signals assigned to the β-hydrogens of the pyridyl groups, the average degree of oligomerization (n) of {(facac)$_2$Zn·**1**}$_n$ can be estimated as 7. The proton signal from the facac groups separates into three distinct resonances. Again, the low-field, minor resonance at 6.05 ppm is likely due to an end group with a singly coordinated zinc fragment. The two larger signals suggest that there is a mixture of products in solution.

The low-temperature ^{1}H NMR spectrum of {(facac)$_2$Zn·**2**}$_n$ is less informative. The only proton signal from **2** that shows a significant downfield shift on coordination is the β-hydrogen signal. However, if on cooling this signal separates to reveal an end group, it is likely that this resonance is buried underneath the other aromatic signals. The singlet from the facac groups remains unchanged, although there is a very small signal at 6.05 ppm, upfield from the main resonance, which may correspond to an end group (see Figure 9).

The two polymers' solution structures were further studied by electrospray mass spectroscopy. This clearly showed their oligomeric nature in solution. The data are presented in Tables 5 and 6. Singly charged ions with chain lengths as great as 5 were observed for both polymers (e.g., [(facac)$_9$Zn$_5$·**1**$_5$]$^+$). Also, doubly charged ions were observed for each polymer that contained as many as 10 zinc units (e.g., [(facac)$_{18}$Zn$_{10}$·**1**$_{11}$]$^{2+}$).

Chiral Polymers. In an attempt to prepare a homochiral analogue of the racemic helical polymer {(facac)$_2$Zn·**1**}$_n$, (+)-3-(trifluoroacetyl)camphor was used as a chiral auxiliary. The corresponding zinc complex was easily prepared as shown in eq 3.

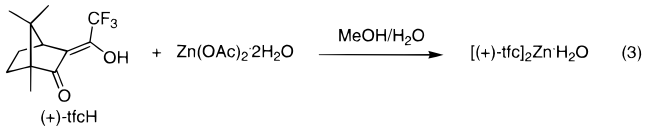

The furanyl linker **1** and [(+)-tfc]$_2$Zn·H$_2$O were reacted in benzene. Crystals of a 1:1 coordination polymer were obtained by slow diffusion of hexane into this solution. Crystallography revealed that this polymer is not helical. Instead of giving the expected cis coordination of the pyridyl groups, the [(+)-tfc]$_2$Zn fragment binds the pyridyl groups in a trans configuration. The resultant polymer has a linear, zigzag structure (see Figure 10). The asymmetric unit of the crystal is two polymer segments long (see Table 7 and 8). Each of the two unique furanyl linkers has a significantly expanded bite angle relative to that of the free ligand (135.4 and 137.6°, respectively). The distortion is evident in a slight bending about the acetylenic units. The two unique zinc centers have an identical binding mode for the (+)-

Table 5. Electrospray Mass Spectroscopy Data (amu) for $\{(facac)_2Zn\cdot\mathbf{1}\}_n$

ion	found	simulated	ion	found	simulated
$[(facac)Zn\cdot\mathbf{1}]^+$	541.4	541.0	$[(facac)_6Zn_4\cdot\mathbf{1}_5]^{2+}$	1427.3	1428.5
$[(facac)_3Zn_2\cdot\mathbf{1}_2]^+$	1293.4	1293.0	$[(facac)_8Zn_5\cdot\mathbf{1}_6]^{2+}$	1802.2	1803.5
$[(facac)_5Zn_3\cdot\mathbf{1}_3]^+$	2041.4	2041.0	$[(facac)_{10}Zn_6\cdot\mathbf{1}_7]^{2+}$	2177.5	2178.0
$[(facac)_7Zn_4\cdot\mathbf{1}_4]^+$	2791.6	2792.0	$[(facac)_{12}Zn_7\cdot\mathbf{1}_7]^{2+}$	2552.8	2553.0
$[(facac)_9Zn_5\cdot\mathbf{1}_5]^+$	3541.6	3540.9	$[(facac)_{14}Zn_8\cdot\mathbf{1}_9]^{2+}$	2927.1	2928.0
$[(facac)Zn\cdot\mathbf{1}_2]^+$	810.9	811.1	$[(facac)_{16}Zn_9\cdot\mathbf{1}_{10}]^{2+}$	3301.8	3303.0
$[(facac)_3Zn_2\cdot\mathbf{1}_3]^+$	1562.7	1563.1	$[(facac)_{18}Zn_{10}\cdot\mathbf{1}_{11}]^{2+}$	3676.8	3678.0

Table 6. Electrospray Mass Spectroscopy Data (amu) for $\{(facac)_2Zn\cdot\mathbf{2}\}_n$

ion	found	simulated	ion	found	simulated
$[(facac)Zn\cdot\mathbf{2}]^+$	551.0	551.0	$[(facac)_3Zn_2\cdot\mathbf{2}_3]^+$	1592.7	1593.1
$[(facac)_3Zn_2\cdot\mathbf{2}_2]^+$	1312.8	1313.0	$[(facac)_5Zn_3\cdot\mathbf{2}_4]^+$	2351.7	2352.1
$[(facac)_5Zn_3\cdot\mathbf{2}_3]^+$	2070.7	2071.0	$[(facac)_7Zn_4\cdot\mathbf{2}_5]^+$	3113.2	3113.1
$[(facac)_7Zn_4\cdot\mathbf{2}_4]^+$	2830.5	2831.0	$[(facac)_{14}Zn_8\cdot\mathbf{2}_9]^{2+}$	2972.1	2973.1
$[(facac)_9Zn_5\cdot\mathbf{2}_5]^+$	3592.3	3592.0	$[(facac)_{16}Zn_9\cdot\mathbf{2}_{10}]^{2+}$	3351.3	3353.1
$[(facac)Zn\cdot\mathbf{2}_2]^+$	833.1	833.1	$[(facac)_{18}Zn_{10}\cdot\mathbf{2}_{11}]^{2+}$	3732.1	3373.1

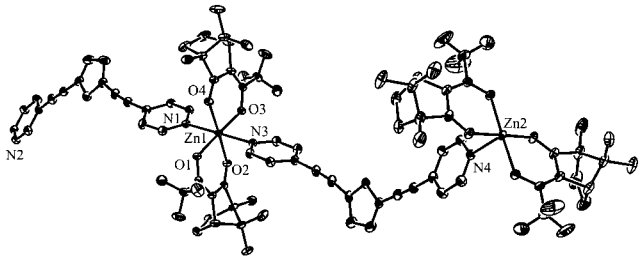

Figure 10. ORTEP diagram of the asymmetric unit of $\{[(+)\text{-tfc}]_2Zn\cdot\mathbf{1}\}_n$ with 50% thermal ellipsoids.

Table 7. Crystallographic Data for $\{[(+)\text{-tfc}]_2Zn\cdot\mathbf{1}\}_n$

empirical formula	$C_{90}H_{82}F_{12}N_4O_{10}Zn_2$
fw	1738.34
temperature	200(0.1) K
wavelength	0.710 73 Å
crystal system	triclinic
space group	$P\bar{1}$
unit cell dimensions	$a = 7.4883(2)$ Å, $b = 14.1563(5)$ Å, $c = 21.2123(5)$ Å, $\alpha = 78.4440(15)°$, $\beta = 81.5644(15)°$, $\gamma = 76.4976(13)°$
volume	2130.35(11) Å^3
Z	1
density (calcd)	1.355 Mg/m^3
abs coeff	0.649 mm^{-1}
θ range for data collection	3.54−31.89°
final R indices $[I > 2\sigma(I)]^a$	R1 = 0.0501, wR2 = 0.1148
R indices (all data)^a	R1 = 0.0746, wR2 = 0.1278

^{a} $R1 = \sum||F_o| - |F_c||/\sum|F_o|$; $wR2 = [\sum w(F_o^2 - F_c^2)^2/\sum w(F_o^2)^2]\}^{1/2}$.

Table 8. Selected Bond Lengths (Å) and Angles (deg) for $\{[(+)\text{-tfc}]_2Zn\cdot\mathbf{1}\}_n$

Zn(1)−N(1)	2.202(3)	Zn(1)−O(1)	2.045(3)	Zn(1)−O(3)	2.057(3)
Zn(1)−N(3)	2.212(3)	Zn(1)−O(2)	2.107(2)	Zn(1)−O(4)	2.109(3)
N1−Zn1−N3		179.2(1)			

tfc ligands (vide supra). In both cases, an anti binding mode is observed, meaning that the trifluoroacetyl fragments are bound anti to one another. Consecutive zinc centers in the polymer are organized in a head-to-tail manner.

Realizing that the $[(+)\text{-tfc}]_2Zn$ fragment could act as a chiral, linear linker, we reacted it with tris(4-pyridyl)methanol (**3**). The

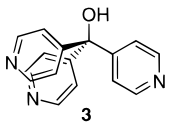

3

hope was to prepare a chiral, neutral dodecahedron, analogous to one reported previously using a bis(platinum) linear linker.[31] Upon the reaction of $[(+)\text{-tfc}]_2Zn\cdot H_2O$ with **3** in the required 3:2 ratio, crystals were in fact grown of a coordination polymer resulting from a 1:1 combination of the two reactants. Ironically, in this case, the pyridyl groups are cis-bound to the zinc fragments, resulting in a helical polymer (see Figure 11). Each metal center has a Λ configuration, producing a right-handed helix. However, alternating metal centers have different coordination environments. In half of the zinc centers, the trifluoroacetyl groups of the (+)-tfc ligands are anti to one another, and in the other half, they are syn to one another (vide supra). There is a single unique tris(4-pyridyl)methanol ligand in the crystal (see Tables 9 and 10). The bond angles about the central carbon atom (C30) deviate slightly from an idealized tetrahedral geometry. The angles about this atom range from 107.1° for the O5−C30−C31 angle to 111.8° for the C27−C30−C36 angle. There is an even greater distortion when the bite angle of the ligand is measured, between the two zinc-bound nitrogen atoms and the central carbon. This angle is 114.3°. The angle between the two zinc atoms and the central carbon is even wider, at 119.1°.

The cause of the surprising 1:1 combination of **3** with $[(+)\text{-tfc}]_2Zn$ can be seen in Figure 12, a stacking diagram viewed down the polymer axes. The remaining pyridyl groups that are not bound to zinc atoms are engaged in hydrogen bonding with the hydroxyl groups of adjacent polymer chains, resulting in a cross-linking of each polymer chain with four of its six neighbors. There are diamond-shaped microchannels running down the length of each helix. The approximate diagonal dimensions are 7.4 × 7.0 Å. The channels are empty, as the equivalent of ether molecules in the crystal occupy positions outside the channels.

Discussion

Both of the new bis(pyridyl) linkers **1** and **2** react with $(facac)_2Zn\cdot 2H_2O$ to yield, upon crystallization, coordination polymers. In each case, a discrete macrocycle could have formed instead. For the reaction of **1**, a distorted hexagon would have been the most likely such product. The sum of the interior angles of a hexagon is 720°. Assuming a coordination angle at the zinc centers of ∼100°, this would require a bis(pyridyl) linker with a bite angle of ∼140°. The natural angle of the furanyl linker **1** was less than anticipated (127°). However, it is flexible due to the acetylenic bridges and can adopt wider bite angles.

(31) Olenyuk, B.; Levin, M. D.; Whiteford, J. A.; Shield, J. E.; Stang, P. J. *J. Am. Chem. Soc.* **1999**, *121*, 10434.

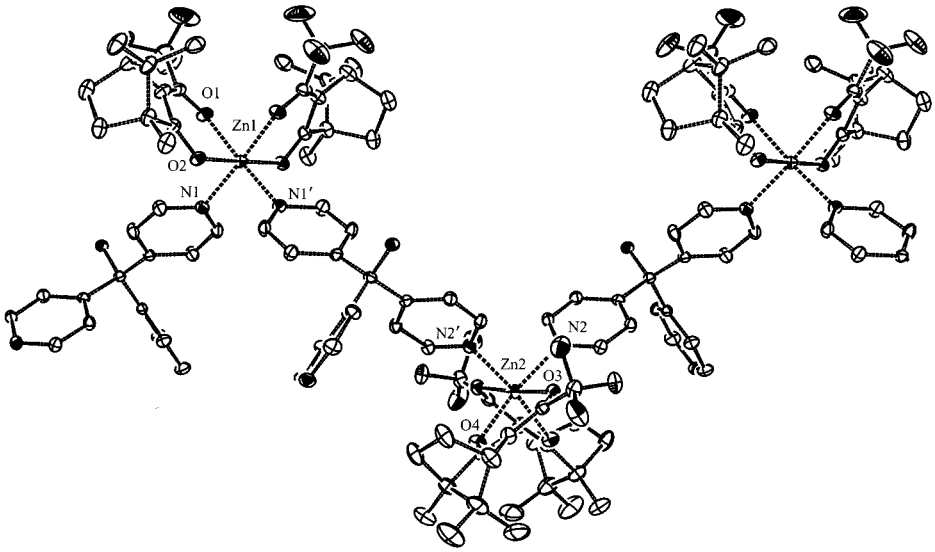

Figure 11. ORTEP diagram of $\{[(+)\text{-tfc}]_2\text{Zn}\cdot\mathbf{3}\}_n$ with 25% thermal ellipsoids.

Table 9. Crystallographic Data for $\{[(+)\text{-tfc}]_2\text{Zn}\cdot\mathbf{3}\}_n$

empirical formula	$C_{44}H_{51}F_6N_3O_6Zn$
fw	897.25
temperature	200(0.1) K
wavelength	0.710 73 Å
crystal system	monoclinic
space group	*C*2
unit cell dimensions	$a = 25.0633(12)$ Å, $b = 11.8768(7)$ Å, $c = 17.1205(9)$ Å, $\alpha = 90°$, $\beta = 117.954(3)°$, $\gamma = 90°$
volume	4501.7(4) Å^3
Z	4
density (calcd)	1.324 Mg/m^3
abs coeff	0.618 mm^{-1}
θ range for data collection	3.25−32.55°
final *R* indices $[I > 2\sigma(I)]^a$	R1 = 0.0593, wR2 = 0.1214
R indices (all data)^a	R1 = 0.1014, wR2 = 0.1398

^{a} $\text{R1} = \sum||F_o| - |F_c||/\sum|F_o|$; $\text{wR2} = [\sum w(F_o^2 - F_c^2)^2/\sum w(F_o^2)^2]^{1/2}$.

For $\{(\text{facac})_2\text{Zn}\cdot\mathbf{1}\}_n$, this angle is 132°, and in $[(+)\text{-tfc}]_2\text{Zn}\cdot\mathbf{1}$, the linker adopts a bite angle as wide as ∼138°. The open, helical structure that was obtained is somewhat similar to the structures of helical oligomers prepared by both Lehn[21] and Moore et al.[22,23] The design of these systems was based on repeating, rigid units with consecutive 120° turns.[24] In the case of $\{(\text{facac})_2\text{Zn}\cdot\mathbf{2}\}_n$, a closed butterfly-type structure could have formed. The approximate sum of the interior angles of such a macrocycle would be 320°, precluding the formation of a square. The solid-state structure of $\{(\text{facac})_2\text{Zn}\cdot\mathbf{2}\}_n$ reflects this butterfly geometry, as revealed in the view of the polymer down its axis (Figure 5).

Small, upfield signals are seen in the low-temperature ^{1}H NMR spectrum of $\{(\text{facac})_2\text{Zn}\cdot\mathbf{1}\}_n$ which are consistent with end groups of the oligomers in solution. It is clear that, in solution, the average value of *n* is at most 7. A puzzling observation is that the proton resonance of the facac groups separates further into two signals of comparable intensities. There are many interpretations for this. One possibility is that, in solution, the oligomers are atactic, giving rise to multiple signals. The crystal structure of this complex reveals that it is unlikely that, in solution, these oligomers could maintain a highly ordered microstructure. Consecutive zinc centers in the helical polymer $\{(\text{facac})_2\text{Zn}\cdot\mathbf{1}\}_n$ are separated by 18.9 Å, due to the wide bite angle of **1**. There are no close contacts between adjacent turns in the helix. As mentioned earlier, Moore et al.[22,23] have prepared oligomers which, in polar solvents, organize to form a helical structure. The driving force for this appears to be π-stacking interactions between consecutive turns in the helix. Such interactions do not seem possible for $\{(\text{facac})_2\text{Zn}\cdot\mathbf{1}\}_n$. As it is, it is unlikely that the oligomers of $\{(\text{facac})_2\text{Zn}\cdot\mathbf{1}\}_n$ even maintain an isotactic microstructure because there appears to be no mechanism for the transfer of stereochemical information between adjacent zinc centers in the chain. The self-assembly processes which lead to the isotactic, helical structure of $\{(\text{facac})_2\text{Zn}\cdot\mathbf{1}\}_n$ in the solid state likely arise during crystallization.

The results from the low-temperature ^{1}H NMR experiment with $\{(\text{facac})_2\text{Zn}\cdot\mathbf{2}\}_n$ are less conclusive. The only observation that can be made is that there is a small signal at 6.05 ppm, upfield from the main facac proton resonance. This may also represent the zinc terminus of the oligomers. From electrospray mass spectroscopy, it is clear that this material exists as a mixture of oligomers in solution.

The preparation of chiral coordination polymers with $[(+)\text{-tfc}]_2\text{Zn}$ is complicated by the many different ways in which this fragment can coordinate two pyridyl groups. Due to the lack of symmetry of the (+)-tfc ligand, there are eight different coordination modes, two with the pyridyl groups bound trans and six with them bound cis. These are shown schematically in Figure 13 (excluding the three structures with a Δ configuration). Three of these binding modes are found in the polymers presented in this paper. The zigzag polymer $\{[(+)\text{-tfc}]_2\text{Zn}\cdot\mathbf{1}\}_n$ was found to adopt a trans-syn configuration at the zinc centers. The trans coordination of the pyridyl groups precluded the formation of a helical polymer. On the other hand, the helical polymer $\{[(+)\text{-tfc}]_2\text{Zn}\cdot\mathbf{3}\}_n$ is composed of alternating zinc centers with Λ-syn and Λ-anti configurations.

The most noteworthy feature of the chiral, helical polymer $\{[(+)\text{-tfc}]_2\text{Zn}\cdot\mathbf{3}\}_n$ is that each polymer chain is cross-linked to four of its neighboring chains by a series of hydrogen bonds. This produces a rare example of a chiral, three-dimensional network polymer with empty microchannels. Solids of this type are much sought after for applications such as inclusion chemistry and catalysis.[32,33] This is also a rare example of a

(32) Joy, A.; Uppili, S.; Netherton, M. R.; Scheffer, J. R.; Ramamurthy, V. *J. Am. Chem. Soc.* **2000**, *122*, 728.
(33) Joy, A.; Scheffer, J. R.; Ramamurthy, V. *Org. Lett.* **2000**, *2*, 119.

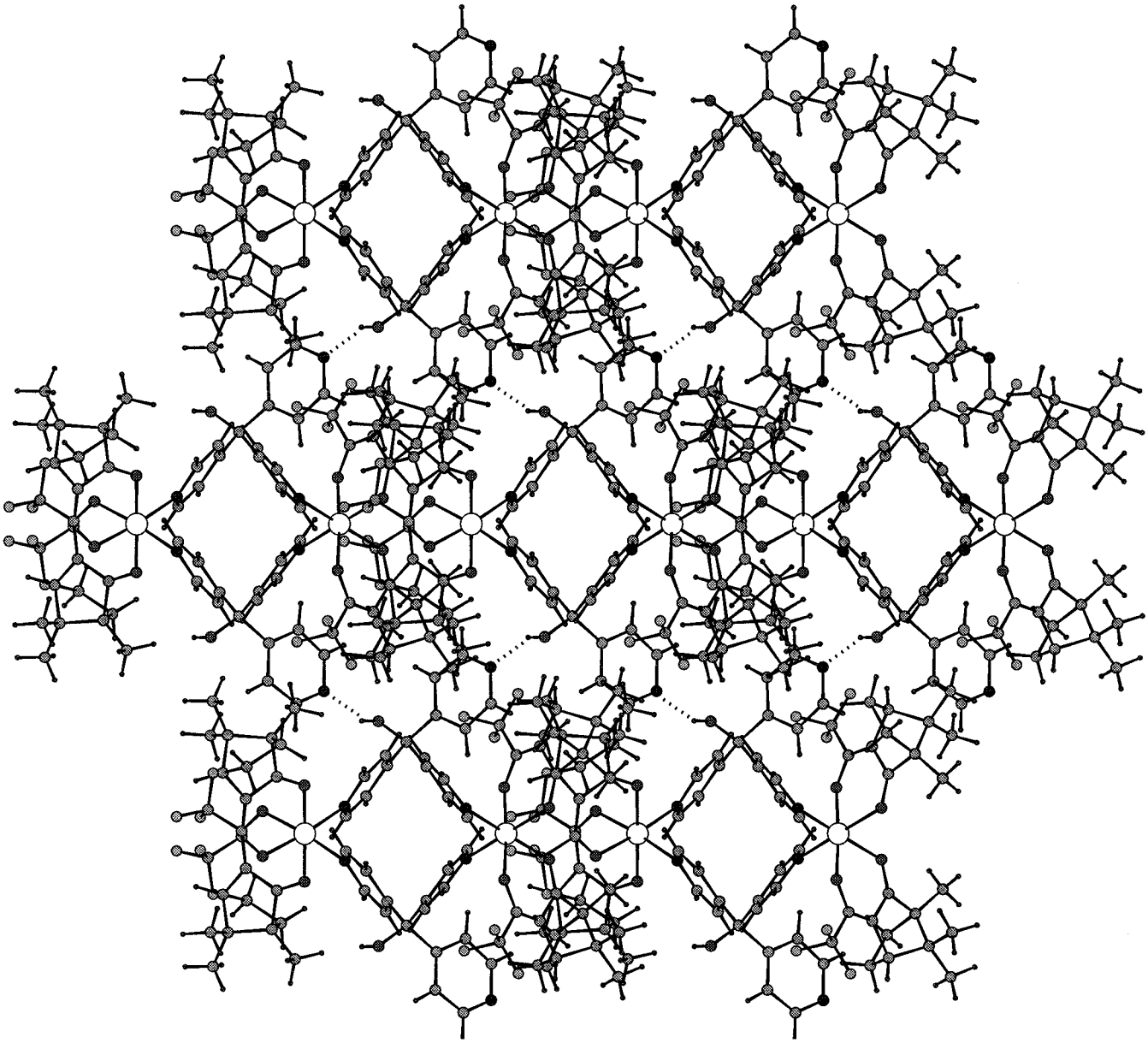

Figure 12. Packing diagram of $\{[(+)\text{-tfc}]_2\text{Zn}\cdot\mathbf{3}\}_n$. Seven polymer chains are shown, viewed down their main axes and revealing diamond-shaped microchannels. The central polymer is cross-linked to its four diagonal neighbors by hydrogen bonds. Hydrogen bonds are shown by dotted lines.

Table 10. Selected Bond Lengths (Å) and Angles (deg) for $\{[(+)\text{-tfc}]_2\text{Zn}\cdot\mathbf{3}\}_n$

Zn(1)−N(1)	2.158(3)	Zn(1)−O(2)	2.068(2)	Zn(2)−O(3)	2.032(2)
Zn(1)−O(1)	2.090(3)	Zn(2)−N(2)	2.191(3)	Zn(2)−O(4)	2.116(3)
N(1)−Zn(1)−N(1)′		97.6(2)	N(2)−Zn(1)−N(2)′		97.9(2)

network polymer composed of both dative-bonding and hydrogen-bonding motifs.[34]

Little information about the structure of the bis(pyridyl) zinc complexes discussed in this paper is revealed in the room-temperature ^{1}H and ^{19}F NMR spectra. For instance, observation of a lone singlet in the ^{19}F spectra of both $\{(\text{facac})_2\text{Zn}\cdot\mathbf{1}\}_n$ and $\{(\text{facac})_2\text{Zn}\cdot\mathbf{2}\}_n$ might at first suggest a trans coordination of the pyridyl groups to the zinc centers in solution.[35−37] This, coupled with their simple ^{1}H NMR spectra, might imply that highly symmetrical macrocycles were present in solution

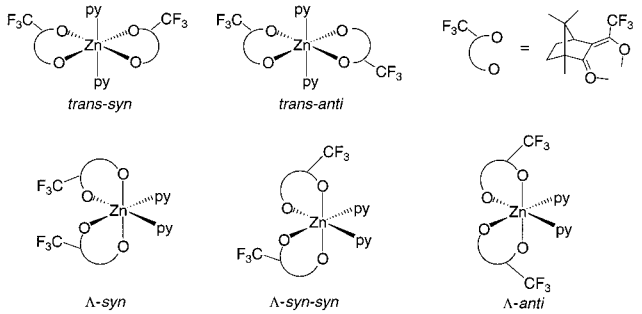

Figure 13. Possible structures of bis(pyridyl) complexes of $\{[(+)\text{-tfc}]_2\text{Zn}$ (excluding Δ configurations).

(34) Ranford, J. D.; Vittal, J. J.; Wu, D.; Yang, X. *Angew. Chem., Int. Ed. Engl.* **1999**, *38*, 3498.
(35) Belford, R. C. E.; Fenton, D. E.; Truter, M. R. *J. Chem. Soc., Dalton Trans.* **1974**, 17.
(36) Adams, R. P.; Allen, H. C.; Rychlewska, U.; Hodgson, D. *J. Inorg. Chim. Acta* **1986**, *119*, 67.
(37) Adams, H.; Bailey, N. A.; Fenton, D. E.; Khalil, R. A. *Inorg. Chim. Acta* **1993**, *209*, 55.

(presumably a triangle and a hexagon or heptagon). However, the low-temperature ^{1}H and ^{19}F spectra reveal dynamic processes that average the signals of quasi-axial and equatorial CF_3 groups, as well as those of different pyridyl groups present in solution. The rapid equilibration of free pyridine with $(facac)_2Zn\cdot 2py$ at room temperature suggests that the pyridyl−zinc linkage is relatively weak. This is supported by the observation that the tripodal linker **3** chooses to engage in hydrogen bonding as well as coordination to zinc in the solid-state structure of $\{[(+)\text{-tfc}]_2Zn\cdot\mathbf{3}\}_n$, suggesting that the zinc−pyridyl bonding interaction is approximately as strong as a hydrogen bond. This may explain why neither $\{(facac)_2Zn\cdot\mathbf{1}\}_n$ nor $\{(facac)_2Zn\cdot\mathbf{2}\}_n$ (or either of the chiral polymers) adopts a closed structure, as the enthalpy gain for forming a macrocycle is not sufficient to overcome the overall loss in entropy during macrocyclization.

Conclusion

In this report, we have shown that the architecture and microstructure of self-assembled, crystalline coordination polymers can be varied by changing the bite angle of bridging, bis(pyridyl) linkers. As noted earlier, the designed synthesis of helical structures is a common goal in supramolecular chemistry. However, the preparation of syndiotactic polymers is less well developed, and the results presented here may help in the further design of syndiotactic systems. The solution structures of the corresponding oligomers of these polymeric solids is certainly more difficult to describe. However, it appears likely that oligomers of $\{(facac)_2Zn\cdot\mathbf{1}\}_n$ are neither isotactic nor helical in solution, despite the structure of the crystalline polymer.

Preparing chiral polymers, and in particular homochiral helices, presents more of a challenge. Although the results were certainly unpredictable, due largely to the dissymmetry of the (+)-tfc ligand, the $[(+)\text{-tfc}]_2Zn$ linking unit did eventually lead to the preparation of a homochiral helical polymer.

Experimental Section

Materials and Methods. NMR spectra were recorded on a Varian XL-300 or a Unity 300 spectrometer. Proton chemical shifts are reported relative to residual protons in acetone-d_6 (2.05 ppm) and C_6D_6 (7.15 ppm). ^{13}C chemical shifts are reported relative to $^{13}CDCl_3$ (77.0 ppm), and ^{19}F chemical shifts are reported relative to an unlocked, external sample of $CFCl_3$ (0.0 ppm). Electrospray mass spectra were obtained with a Micromass Quatro II with ionization performed under electrospray conditions (flow rate 7.7 μL/min, capillary voltage 3.0 kV, cone voltage 70 V, extractor voltage 16 V). Fifteen individual scans were averaged for the mass spectrum. The calibration of the mass range 500−4000 amu was done with a 1:1 mixture of a 2-propanol−water solution of NaI (2 μg/μL) and CsI (0.01 μg/μL). Samples were prepared as 0.02 mmol/L solutions in a 1:1 acetone−methylene chloride solution just prior to analysis. Elemental analyses were performed by Atlantic Microlab, Norcross, GA. Melting points are uncorrected.

All solvents were of reagent grade and were used as received, except for triethylamine, THF, and $CDCl_3$. Triethylamine was distilled from KOH immediately before use, and likewise THF was distilled from Na/benzophenone. $CDCl_3$ was filtered through basic alumina before use. Flash chromatography was performed on 230−400 mesh, 60 Å silica gel (Baxter).

All reagents were purchased from Aldrich, except for $(Ph_3P)_2PdCl_2$, which was purchased from Lancaster. 2,5-Dibromofuran,[38] 4-ethynylpyridine,[39] and tris(4-pyridyl)methanol (**3**) were prepared according to literature methods.

Preparations. 2,5-Bis(4-ethynylpyridyl)furan, 1. Triethylamine (10 mL) was distilled into a calibrated 50 mL Schlenk flask. To this were added, under an argon flush, $(Ph_3P)_2PdCl_2$ (27.9 mg, 0.04 mmol) and CuI (7.7 mg, 0.04 mmol), giving a yellow suspension. Next, 2,5-dibromofuran (0.41 g, 0.17 mL, 1.8 mmol) was added via syringe, followed by 4-ethynylpyridine (0.4873 g, 4.7 mmol). Finally, THF (10 mL) was added, taking care to wash down the sides of the flask. On stirring, the solution turned orange. The mixture was heated in the dark to 70 °C for 17 h. On cooling and standing, a brown precipitate rapidly settled, giving an orange supernate. The mixture was then concentrated in vacuo to give a brown solid. The solid was extracted with several portions of Et_2O, and the extracts were filtered through Celite. On concentration, 0.62 g crude orange solid was obtained. The product was dissolved in a minimal amount of CH_2Cl_2, and the solution was flash-chromatographed through silica gel (10 g), using Et_2O as the eluant. A white solid (0.42 g) was obtained. The solid was dissolved in warm CH_2Cl_2, and the solution was filtered. Hexanes were added, and the mixture was refluxed on a steam bath until small needles began to form. After the mixture was allowed to stand overnight, the crystals were collected on a frit, washed with hexanes, and dried in vacuo. A 0.3286 g quantity (67% yield) of **1** was obtained. Crystals for X-ray diffraction were grown by storing a saturated solution of **1** in acetone at −15 °C overnight. ^{1}H NMR (300 MHz, acetone-d_6): δ 8.67 (dd, J = 4.3, 1.6 Hz, 4 H), 7.52 (dd, H = 4.3, 1.6 Hz, 4 H), 7.06 (s, 2 H). ^{13}C NMR (75 MHz, $CDCl_3$): δ 149.9, 137.5, 129.9, 125.0, 118.0, 91.9, 83.1. Anal. Calcd for $C_{18}H_{10}N_2O$: C, 79.99; H, 3.73; N, 10.36. Found: C, 80.04; H, 3.61; N, 10.04.

1,2-Bis(4-ethynylpyridyl)benzene, 2. Triethylamine (25 mL) was distilled into a calibrated 50 mL Schlenk flask under argon. To this were added 1,2-diiodobenzene (640 mg, 0.25 mL, 1.9 mmol), 4-ethynylpyridine (503.5 mg, 4.88 mmol), $(Ph_3P)_2PdCl_2$ (30.5 mg, 0.043 mmol), and CuI (9.2 mg, 0.048 mmol). The light yellow mixture was stirred at room temperature in the dark for 22 h. A white precipitate formed and settled easily. The mixture was concentrated in vacuo and extracted with several portions of Et_2O, and the extracts were filtered through Celite. On concentration, a crude yellow solid (0.65 g) was obtained. The solid was extracted into several portions of boiling hexanes, and the extracts were filtered through Celite (total volume ~200 mL). After standing overnight at −15 °C, the flask was filled with white fluffy crystals. The mother liquor was removed by cannula filtration, while the mixture was kept at −10 °C with an ethanol/ice bath. The white solid was washed with two portions of cold hexanes (100 mL, 50 mL). After the solid was dried in vacuo, 0.3645 g (67% yield) of **2** was obtained as a white, fluffy solid. ^{1}H NMR (300 MHz, acetone-d_6): δ 8.65 (dd, J = 4.4, 1.7 Hz, 4 H), 7.73 (dd, J = 5.9, 3.5 Hz, 2 H), 7.55 (dd, J = 5.9, 3.5 Hz, 2 H), 7.52 (dd, J = 4.4, 1.7 Hz, 4 H). ^{13}C NMR (75 MHz, $CDCl_3$): δ 149.9, 132.2, 131.1, 129.0, 125.4, 124.9, 92.2, 90.9. Anal. Calcd for $C_{20}H_{12}N_2$: C, 85.69; H, 4.31; N, 10.01. Found: C, 85.58; H, 4.27; N, 10.08.

$[(+)\text{-tfc}]_2Zn\cdot H_2O$. To a pink solution of (+)-tfcH (0.9844 g, 3.97 mmol) in warm methanol (4 mL) was added a hot aqueous solution (10 mL) of $Zn(OAc)_2\cdot 2H_2O$ (0.4353 g, 1.98 mmol). The mixture was washed with two 2 mL portions of water. A white, sticky solid immediately formed. The mixture was rapidly stirred and then heated to reflux for 10 min. When necessary, a spatula was used to break up the solid. Next, the solid was collected on a coarse frit, and washed with excess water. On drying, 0.9740 g of crude product was obtained (85% yield). This material was dissolved in hot methanol, and the solution was filtered. While the filtrate was heated on a steam bath, hot water was slowly added until crystals began to form. On cooling and standing, the flask became filled with white needles. These were collected, washed with several portions of water, and dried in vacuo. A 0.8590 g quantity of $[(+)\text{-tfc}]_2Zn\cdot H_2O$ was obtained (75% yield). ^{1}H NMR (300 MHz, C_6D_6): δ 2.76 (quintet, J = 2.9 Hz, 2 H), 2.62 (br s, 2 H (bound H_2O)), 1.70 (m, 2 H), 1.31 (m, 6 H), 0.85 (s, 6 H), 0.77 (s, 6 H), 0.53 (s, 6 H). ^{19}F NMR (282 MHz, C_6D_6): δ −68.13 (s). $[\alpha]^{26°C}_D$ = +175° (10 cm, c = 0.5 g/100 mL ($CHCl_3$)). Anal. Calcd for $C_{24}H_{28}F_6O_4Zn\cdot H_2O$: C, 49.88; H, 5.23. Found: C, 49.80; H, 5.13.

$\{(facac)_2Zn\cdot\mathbf{1}\}_n$. In a 50 mL round-bottom flask, $(facac)_2Zn\cdot 2H_2O$ (18.7 mg, 0.0363 mmol) was dissolved in acetone (6 mL). To this was added a solution of **1** (9.8 mg, 0.036 mmol) in acetone (2 mL), with three subsequent acetone washes (1, 1, 0.5 mL). The solution was refluxed on a steam bath. Toluene (10 mL) was added, and the solution

(38) Keegstra, M. A.; Klomp, A. J. A.; Brandsma, L. *Synth. Commun.* **1990**, *20*, 3371.
(39) Ciana, L. D.; Haim, A. *J. Heterocycl. Chem.* **1984**, *21*, 607.

was heated until refluxing subsided. The flask was covered with a Kimwipe and allowed to sit in the dark for several days, during which large crystals appeared. The mother liquor was decanted, and the crystals were washed with toluene (twice) and hexanes (twice). After the solid was dried in vacuo, 19.1 mg of $\{(facac)_2Zn\cdot\mathbf{1}\}_n$ (70% yield) was obtained as a white powder. ^{1}H NMR (300 MHz, acetone-d_6): δ 8.70 (d, J = 6.3 Hz, 4 H), 7.75 (d, J = 6.3 Hz, 4 H), 7.13 (s, 2 H), 6.02 (s, 2 H). ^{19}F NMR (282 MHz, acetone-d_6): room temperature, δ −76.82 (s); −80 °C, δ −75.70 (s), −76.29 (s). Mp: 260 °C dec. Anal. Calcd for $C_{28}H_{12}F_{12}N_2O_5Zn$: C, 44.85; H, 1.61; N, 3.74. Found: C, 44.89; H, 1.61; N, 3.73.

$\{(facac)_2Zn\cdot\mathbf{2}\}_n$. To a 3 mL vial were added **2** (15.6 mg, 0.0556 mmol) and $(facac)_2Zn\cdot 2H_2O$ (28.9 mg, 0.0560 mmol). The mixture was dissolved in acetone (2 mL), with stirring. The stir bar was removed, and the solution was washed with a small portion of acetone (0.5 mL). The vial was sealed in a small bottle containing pentane and allowed to stand. After several days, large colorless crystals had grown. The mother liquor was decanted, and the crystals were washed three times with ether. After the solid was dried in vacuo, 37.4 mg (88% yield) of $\{(facac)_2Zn\cdot\mathbf{2}\}_n$ was obtained. ^{1}H NMR (300 MHz, acetone-d_6): δ 8.66 (dd, J = 4.9, 1.6 Hz, 4 H), 7.82 (dd, J = 4.9, 1.6 Hz, 4 H), 7.77 (dd, J = 5.9, 3.4 Hz, 2 H), 7.61 (dd, J = 5.9, 3.4 Hz, 2 H), 6.01 (s, 2 H). ^{19}F NMR (282 MHz, acetone-d_6): room temperature, δ −76.49 (s); −80 °C, δ −75.56 (s), −76.19 (s). Mp: 260 °C dec. Anal. Calcd for $C_{30}H_{14}F_{12}N_2O_4Zn$: C, 47.42; H, 1.86; N, 3.69. Found: C, 47.50; H, 1.90; N, 3.73.

$\{[(+)\text{-(tfc)}]_2Zn\cdot\mathbf{1}\}_n$. Benzene was added to a mixture of **1** (14.2 mg, 0.0525 mmol) and $[(+)\text{-tfc}]_2Zn\cdot H_2O$ (30.5 mg, 0.0528 mmol), and the resulting mixture was stirred rapidly until the solids were dissolved. The stir bar was removed, followed by a small benzene wash (1 mL), and the mixture was sealed in a jar of hexanes. After several days, colorless crystals of $\{[(+)\text{-tfc}]_2Zn\cdot\mathbf{1}\}_n\cdot 0.2C_6H_6$ (40.8 mg, 92% yield) were collected, washed with hexanes, and dried in vacuo. Recrystallization by a similar method produced crystals suitable for structure determination. ^{1}H NMR (300 MHz, C_6D_6): δ 8.56 (dd, J = 4.8, 1.5 Hz, 4 H), 6.66 (dd, J = 4.7, 1.6 Hz, 4 H), 6.25(s, 2 H), 2.91 (quintet, J = 3.0 Hz, 2 H), 1.83 (m, 2 H), 1.42 (m, 4 H), 1.28 (m, 2 H), 0.97 (s, 6 H), 0.78 (s, 6 H), 0.62 (s, 6 H), 0.55 (br s, 2 H (unbound H_2O)). ^{19}F NMR (282 MHz, C_6D_6): δ −71.14 (s). Anal. Calcd for $C_{42}H_{38}F_6N_2O_5Zn\cdot 0.2C_6H_6$: C, 61.35; H, 4.67; N, 3.31. Found: C, 61.40; H, 4.79; N, 3.21. Mp: 216−218 °C dec.

$\{[(+)\text{-tfc}]_2Zn\cdot\mathbf{3}\}_n$. To an acetone solution (4 mL) of $[(+)\text{-tfc}]_2Zn\cdot H_2O$ (26.6 mg, 0.0460 mmol) was added a methanol solution (1 mL) of **3** (11.6 mg, 0.0441 mmol), followed by small methanol washes (2 × 0.5 mL). The mixture was rapidly stirred, and the stir bar was removed. Next, the solution was sealed in a jar containing a 1:1 mixture of ether and pentane. After 1 week, colorless crystals of $\{[(+)\text{-tfc}]_2Zn\cdot\mathbf{3}\}_n\cdot 0.5C_4H_{10}O$ (29.4 mg, 78% yield) were collected, washed with ether, and dried in vacuo. Recrystallization by vapor diffusion of an ether−pentane mixture (1:1) into an acetone solution of $\{[(+)\text{-tfc}]_2Zn\cdot\mathbf{3}\}_n$ produced crystals suitable for X-ray diffraction. ^{1}H NMR (300 MHz, C_6D_6): δ 8.62 (dd, J = 4.7, 1.7 Hz, 6 H), 7.43 (dd, J = 4.7, 1.7 Hz, 6 H), 2.73 (quintet, J = 3.0 Hz, 2 H), 2.00 (m, 2 H), 1.65 (m, 2 H), 1.27 (m, 4 H), 0.90 (s, 6 H),), 0.88 (s, 6 H), 0.77 (s, 6 H). ^{19}F NMR (282 MHz, C_6D_6): δ −70.95 (s). Anal. Calcd for $C_{40}H_{41}F_6N_3O_5Zn\cdot 0.5C_4H_{10}O$: C, 58.64; H, 5.39; N, 4.88. Found: C, 58.91; H, 5.33; N, 4.98. Mp: 244−246 °C dec.

Crystal Structure Determinations. $\{(facac)_2Zn\cdot\mathbf{1}\}_n$. A colorless irregularly shaped crystal 0.18 × 0.15 × 0.10 mm in size was mounted on a glass fiber with tiny traces of viscous oil and then transferred to a Nonius KappaCCD diffractometer equipped with Mo Kα radiation (λ = 0.710 73 Å). Ten frames of data were collected at 200(0.1) K with an oscillation range of 1°/frame and an exposure time of 20 s/frame.[40] Indexing and unit cell refinement based on all observed reflections from those 10 frames indicated a monoclinic P lattice. A total of 11 068 reflections (θ_{max} = 26.00°) were indexed, integrated, and corrected for Lorentz, polarization, and absorption effects using DENZO-SMN and SCALEPAC.[41] Postrefinement of the unit cell gave a = 11.0374(3) Å, b = 24.2179(10) Å, c = 14.3970(4) Å, β = 92.880(2)°, and V = 3843.5(2) Å^3. Axial photographs and systematic absences were consistent with the compound having crystallized in the monoclinic space group $P2_1/n$ (No. 14). The structure was solved by a combination of direct and heavy-atom methods using SIR 97.[42] All of the non-hydrogen atoms were refined with anisotropic displacement coefficients. Hydrogen atoms were assigned isotropic displacement coefficients U(H) = 1.2U(C) or 1.5U(C_{methyl}), and their coordinates were allowed to ride on their respective carbons using SHELXL97.[43] The CF_3 groups are disordered into two different orientations with 50:50 occupancy. There are two disordered molecules of toluene associated with the molecule. The weighting scheme employed was $w = 1/[\sigma^2(F_o^2) + (0.0879P)^2 + 3.7902P]$ where $P = (F_o^2 + 2F_c^2)/3$. The refinement converged to R1 = 0.0632, wR2 = 0.1617, and S = 1.032 for 4592 reflections with $I > 2\sigma(I)$ and R1 = 0.1005, wR2 = 0.1852, and S = 1.032 for 6857 unique reflections and 511 parameters.[44] The maximum Δ/σ in the final least-squares cycle was 0.007, and the residual peaks on the final difference Fourier map ranged from −0.358 to 0.475 e/Å^3. Scattering factors were taken from refs 45 and 46.

$\{(facac)_2Zn\cdot\mathbf{2}\}_n$ A colorless prism-shaped crystal 0.20 × 0.15 × 0.10 mm in size was mounted on a glass fiber with tiny traces of viscous oil and then transferred to a Nonius KappaCCD diffractometer equipped with Mo Kα radiation (λ = 0.710 73 Å). Ten frames of data were collected at 200(0.1) K with an oscillation range of 1°/frame and an exposure time of 20 s/frame.[40] Indexing and unit cell refinement based on all observed reflections from those 10 frames indicated a monoclinic P lattice. A total of 13 290 reflections (θ_{max} = 30.00°) were indexed, integrated, and corrected for Lorentz, polarization, and absorption effects using DENZO-SMN and SCALEPAC.[41] Postrefinement of the unit cell gave a = 9.1344(1) Å, b = 21.7985(5) Å, c = 16.0322(4) Å, β = 99.6680(11)°, and V = 3146.93(11) Å^3. Axial photographs and systematic absences were consistent with the compound having crystallized in the monoclinic space group $P2_1/n$ (No.14). The structure was solved by a combination of direct and heavy-atom methods using SIR 97.[42] All of the non-hydrogen atoms were refined with anisotropic displacement coefficients. Hydrogen atoms were assigned isotropic displacement coefficients U(H) = 1.2U(C) or 1.5U(C_{methyl}), and their coordinates were allowed to ride on their respective carbons using SHELXL97.[43] Three CF_3 groups were disordered in two different orientations with partial occupancy ranging from 0.5 to 0.75. The weighting scheme employed was $w = 1/[\sigma^2(F_o^2) + (0.04431P)^2 + 0.9117P]$ where $P = (F_o^2 + 2F_c^2)/3$. The refinement converged to R1 = 0.0464, wR2 = 0.0984, and S = 1.025 for 5968 reflections with $I > 2\sigma(I)$ and to R1 = 0.0852, wR2 = 0.1127, and S = 1.025 for 9011 unique reflections and 526 parameters.[44] The maximum Δ/σ in the final least-squares cycle was 0.077, and the residual peaks on the final difference Fourier map ranged from −0.374 to +0.486 e/Å^3. Scattering factors were taken from refs 45 and 46.

$\{[(+)\text{-tfc}]_2Zn\cdot\mathbf{1}\}_n$. A colorless, thin, plate-shaped crystal 0.3 × 0.25 × 0.08 mm in size was mounted on a glass fiber with tiny traces of viscous oil and then transferred to a Nonius KappaCCD diffractometer equipped with Mo Kα radiation (λ = 0.710 73 Å). Ten frames of data were collected at 200(0.1) K with an oscillation range of 1°/frame and an exposure time of 20 s/frame.[40] Indexing and unit cell refinement

(40) *COLLECT Data Collection Software*; Nonius BV: Delfft, The Netherlands, 1998.

(41) Otwinowski, Z.; Minor, W. Processing of X-ray Diffraction Data Collected in Oscillation Mode. *Methods Enzymol.* **1997**, *276*, 307−326.

(42) Altomare, A.; Burla, M. C.; Camalli, M.; Cascarano, G.; Giacovazzo, C.; Guagliardi, A.; Moliteni, A. G. G.; Polidori, G.; Spagna, R. *SIR97: A program for automatic solution and refinement of crystal structure*, Release 1.02; Bari, Italy, 1997.

(43) SHELX97 (includes SHELXS97, SHELXL97, and CIFTAB): Sheldrick, G. M. *SHELX97: Programs for Crystal Structure Analysis*, Release 97-2; University of Göttingen: Göttingen, Germany, 1997.

(44) $R1 = \sum||F_o| - |F_c||/\sum|F_o|$, $wR2 = [\sum w(F_o^2 - F_c^2)^2/\sum w(F_o^2)^2]^{1/2}$, and S = goodness-of-fit on $F^2 = [\sum w(F_o^2 - F_c^2)^2/(n - p)]^{1/2}$, where n is the number of reflections and p is the number of parameters refined.

(45) Maslen, E. N.; Fox, A. G.; O'Keefe, M. A. In *International Tables for Crystallography*; Wilson, A. J. C., Ed.; Kluwer: Dordrecht, The Netherlands, 1992; Vol. C, pp 476−516.

(46) Creagh, D. C.; McAuley, W. J. In *International Tables for Crystallography*; Wilson, A. J. C., Ed.; Kluwer: Dordrecht, The Netherlands, 1992; Vol. C, Chapter 4, pp 206−222.

based on all observed reflections from those 10 frames indicated a triclinic *P* lattice. A total of 16 950 reflections ($\theta_{max} = 31.89°$) were indexed, integrated, and corrected for Lorentz, polarization, and absorption effects using DENZO-SMN and SCALEPAC.[41] Postrefinement of the unit cell gave $a = 7.4883(2)$ Å, $b = 14.1563(5)$ Å, $c = 21.2123(5)$ Å, $\alpha = 78.4440(15)°$, $\beta = 81.5644(15)°$, $\gamma = 76.4976(13)°$, and $V = 2130.35(11)$ Å^3. Axial photographs and systematic absences were consistent with the compound having crystallized in the triclinic space group *P*1. The structure was solved by a combination of direct and heavy-atom methods using SIR 97.[42] All of the non-hydrogen atoms were refined with anisotropic displacement coefficients. Hydrogen atoms were assigned isotropic displacement coefficients $U(H) = 1.2U(C)$ or $1.5U(C_{methyl})$, and their coordinates were allowed to ride on their respective carbons using SHELXL97.[43] The weighting scheme employed was $w = 1/[\sigma^2(F_o^2) + (0.0591P)^2 + 0.7107P]$ where $P = (F_o^2 + 2F_c^2)/3$. The correct absolute structure was determined using Flack's parameter *X*. The refinement converged to R1 = 0.0501, wR2 = 0.1148, and $S = 1.007$ for 12 996 reflections with $I > 2\sigma(I)$ and to R1 = 0.0746, wR2 = 0.1278, and $S = 1.007$ for 16 950 unique reflections and 1053 parameters.[44] The maximum Δ/σ in the final least-squares cycle was 0.068, and the residual peaks on the final difference Fourier map ranged from −0.515 to +0.952 e/Å^3. Scattering factors were taken from refs 45 and 46.

{[(+)-tfc]$_2$Zn·3}$_n$. A colorless prism-shaped crystal 0.25 × 0.25 × 0.2 mm in size was mounted on a glass fiber with tiny traces of viscous oil and then transferred to a Nonius KappaCCD diffractometer equipped with Mo Kα radiation ($\lambda = 0.710\,73$ Å). Ten frames of data were collected at 200(0.1) K with an oscillation range of 1°/frame and an exposure time of 20 s/frame.[40] Indexing and unit cell refinement based on all observed reflections from those 10 frames indicated a monoclinic *C* lattice. A total of 12 057 reflections ($\theta_{max} = 32.55°$) were indexed, integrated, and corrected for Lorentz, polarization, and absorption effects using DENZO-SMN and SCALEPAC.[41] Postrefinement of the unit cell gave $a = 25.0633(12)$ Å, $b = 11.8768(7)$ Å, $c = 17.1205(9)$ Å, $\beta = 117.954(3)°$, and $V = 4501.7(4)$ Å^3. Axial photographs and systematic absences were consistent with the compound having crystallized in the monoclinic space group *C*2.The structure was solved by a combination of direct and heavy-atom methods using SIR 97.[42] All of the non-hydrogen atoms were refined with anisotropic displacement coefficients. All hydrogen atoms, except H−O5, which was located and refined isotropically, were assigned isotropic displacement coefficients $U(H) = 1.2U(C)$ or $1.5U(C_{methyl})$, and their coordinates were allowed to ride on their respective carbons using SHELXL97.[43] The asymmetric unit contains one molecule of ether solvent. The weighting scheme employed was $w = 1/[\sigma^2(F_o^2) + (0.0487P)^2 + 3.9351P]$ where $P = (F_o^2 + 2F_c^2)/3$. The refinement converged to R1 = 0.0593, wR2 = 0.1214, and $S = 1.018$ for 8242 reflections with $I > 2\sigma(I)$ and to R1 = 0.1014, wR2 = 0.1398, and $S = 1.018$ for 12 057 unique reflections and 548 parameters.[44] The maximum Δ/σ in the final least-squares cycle was 0.006, and the residual peaks on the final difference Fourier map ranged from −0.601 to +0.344 e/Å^3. Scattering factors were taken from refs 45 and 46.

Acknowledgment. Financial support from the NSF (CHE-9818472) is gratefully acknowledged, and M.S. thanks the Alexander von Humboldt Foundation for a Feodor Lynen Fellowship.

Supporting Information Available: Listings of X-ray experimental details, positional and thermal parameters, and bond distances and angles for **1**, {(facac)$_2$Zn·**1**}$_n$, {(facac)$_2$Zn·**2**}$_n$, {[(+)-tfc]$_2$Zn·**1**}$_n$ and {[(+)-tfc]$_2$Zn·**3**}$_n$, along with fully labeled ORTEP diagrams. This material is available free of charge via the Internet at http://pubs.acs.org.

IC991315M